High Power Wideband Gyrotron Backward Wave Oscillator Operating towards the Terahertz Region

W. He, C. R. Donaldson, L. Zhang, K. Ronald, P. McElhinney, and A. W. Cross
Department of Physics, SUPA, University of Strathclyde, Glasgow, G4 0NG, United Kingdom
(Received 28 December 2012; published 15 April 2013)

Experimental results are presented of the first successful gyrotron backward wave oscillator (gyro-BWO) with continuous frequency tuning near the low-terahertz region. A helically corrugated interaction region was used to allow efficient interaction over a wide frequency band at the second harmonic of the electron cyclotron frequency without parasitic output. The gyro-BWO generated a maximum output power of 12 kW when driven by a 40 kV, 1.5 A, annular-shaped large-orbit electron beam and achieved a frequency tuning band of 88–102.5 GHz by adjusting the cavity magnetic field. The performance of the gyro-BWO is consistent with 3D particle-in-cell numerical simulations.

DOI: 10.1103/PhysRevLett.110.165101 PACS numbers: 84.40.Ik, 52.59.Rz

The operation of gyrodevices is based on the cyclotron resonance maser instability of electrons gyrating in an external magnetic field. The instability causes electrons to bunch in the cyclotron phase space and to lose energy to the interacting electromagnetic wave in a coherent and efficient way [1]. Gyrodevices have the capability of high frequency operation into the terahertz range as demonstrated by a number of recent gyrotron experiments [2–6]. However, gyrotrons can only operate at discrete frequencies which limit their applications. Terahertz waves have many exciting applications including plasma diagnostics, remote imaging, and electron spin resonance spectroscopy [7]. These applications can be greatly enhanced if such a source has frequency tunability, for example, allowing the measurement of the plasma density distribution over a volume [8], with higher range resolution [9] and improved sensitivity, resolution, and orientational selectivity in spectroscopy [10]. The potential of gyrotron backward wave oscillators (gyro-BWOs) as a high power (kW) coherent powerful microwave source with wide-frequency tunability has hitherto [11–15] been achieved only at frequencies well below the terahertz range. The exception has been one gyro-BWO operating in the low terahertz range at 140 GHz but this experiment was unable to demonstrate continuous frequency tuning [16]. An encouraging systematic study for operation in the low terahertz range is being carried out in order to mitigate the prevalent problem of parasitic oscillations from undesired modes [17].

This Letter presents the first successful operation of a high power gyro-BWO with a wide frequency tuning capability in the low terahertz frequency range. A novel helically corrugated interaction region (HCIR) and thermionic cusp electron gun were used in the gyro-BWO. Stable single mode output was achieved in a wide frequency tuning range of ~16% with a maximum power of 12 kW and an electronic efficiency of 20%.

A schematic outline of the gyro-BWO apparatus is shown in Fig. 1. An electron current of 1.5 A was produced by thermionic emission from an annular shaped cathode and accelerated through a potential difference of 40 kV. This beam passes through a smooth magnetic "cusp" located a few millimeters in the front of the cathode [18] to form an annular shaped large orbit beam as it enters the HCIR cavity in a region of uniform magnetic field [19], where the interaction with the eigenwave field takes place. For this large-orbit beam, optimum coupling for interaction at the harmonic number s occurs with TE_{sn} modes, having the azimuthal index equal to the harmonic number. In the experiment a beam velocity ratio α of 1.6 was chosen so that the beam has sufficient energy in the transverse momentum for extraction as radiation energy. The gyro-BWO was provided with two UHV compliant broadband millimeter wave windows. One, downstream from the interaction waveguide and mounted on the end of a horn antenna took the form of a "three disk" configuration with a reflection coefficient of better than −20 dB [20] and enabled characterization and diagnosis of the radiation generated in the far field of the launcher. Upstream from the HCIR a wideband sidewall coupler was provided as an alternative output port and used to inject or extract the radiation. The coupler was fitted with a brazed ceramic disk in a pillbox structure to

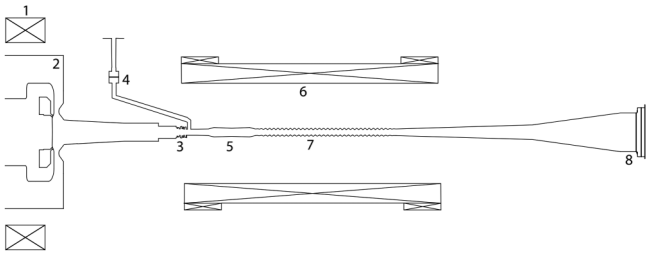

FIG. 1. Gyro-BWO experimental configuration (1: reverse coil, 2: cusp gun, 3: Bragg reflector, 4: output coupler, 5: circular to linear wave converter, 6: cavity coil, 7: HCIR, and 8: three-disk output window).

seal the ultrahigh vacuum. The coupler was designed for enhanced mechanical robustness and larger machining tolerances. To allow maximum beam transportation in the coupler region, a wideband reflector whose minimum diameter is the same as the diameter of the beam tunnel (2.6 mm) was used instead of a cutoff waveguide at the diode side of the coupler to inhibit wave propagation. The coupler was numerically optimized for maximum wave transmission by using MICIAN μWAVE WIZARD and achieved a reflection of better than -10 dB in the frequency band of 84–104 GHz. A wave polarization converter [21] was used to convert the circularly polarized wave radiated from the interaction region to linear polarization so that the signal could be coupled out through the coupler or vice versa.

The HCIR has a helical profile on its inner surface described by $r(\varphi, z) = 1.30 + 0.24\sin(3\varphi - 2\pi z/3.75)$ in cylindrical coordinates (r, φ, z). Here, r and z are in millimeters.

The dispersion of the eigenwaves in a HCIR can be manipulated by adjusting the geometrical shape and dimensions of the HCIR due to the coupling of resonant modes [22]. "Ideal" eigenwaves can therefore be achieved for broadband microwave amplification in a gyrotron traveling wave amplifier [23], wide frequency tuning in a gyro-BWO [24] and high compression ratio in a microwave pulse compressor [25]. In a gyro-BWO the excited radiation frequency is determined by the cyclotron harmonic and the Doppler shift term $\omega = s\omega_c + k_z v_z$. Here, ω is the angular frequency of the radiation, s is the harmonic number, k_z the axial component of the radiation field wave vector and v_z is the electron axial velocity. The relativistic cyclotron frequency, determined by $\omega_c = eB/\gamma m_0$, describes the angular frequency of rotation of the electrons in the axial magnetic field where e/m_0 is the electron charge-mass ratio, $\gamma = 1 + |eV|/m_0c^2$ is the relativistic Lorentz factor for a beam accelerated over a potential difference V, and B is the magnetic induction of the guiding field. A wave may be excited where this frequency is close to the dispersion relation of the HCIR. In this gyro-BWO experiment the HCIR was optimally designed to couple two low order modes: the traveling TE_{11} and the near cutoff TE_{21} modes. The resultant operating wave, which is the lowest eigenwave, has a large, near constant group velocity value of $\sim 0.62c$ (c is the speed of light in vacuum) calculated by perturbation theory [22] and is shown in the dispersion diagram Fig. 2(a). This allows a larger relative frequency-tuning band to be achieved with a linear tuneability of the output frequency against the tuning magnetic field. Operating on the lowest eigenwave eliminates the possibility of parasitic oscillations. Efficient beam-wave interaction takes place only in a region of sufficiently small k_z because the spread in v_z causes the broadening of the cyclotron line and weakening of the resonance between the beam and the wave.

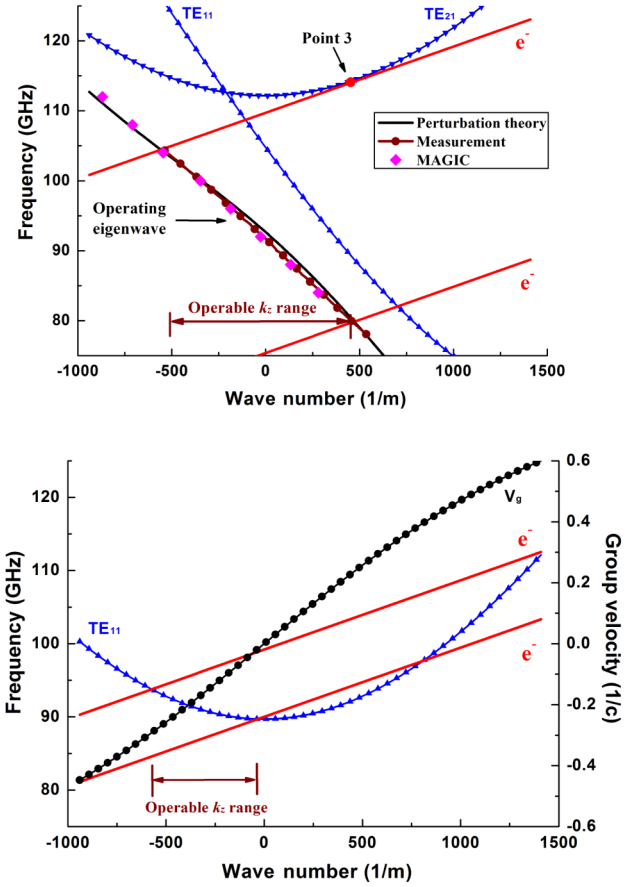

FIG. 2 (color online). (a) Dispersion diagram of the operating eigenwave (analytical, simulated, and measured), the second harmonic electron cyclotron mode (e^-), and (b) dispersion diagram of a smooth circular waveguide gyro-BWO.

As a comparison the dispersion diagram of a conventional smooth bore cylindrical cavity gyro-BWO is shown in Fig. 2(b). For efficient stable single mode operation it should also operate on the lowest TE_{11} mode interacting with the fundamental electron cyclotron mode. The dispersion of a wave in cylindrical waveguide can be expressed as $\omega^2 = c^2k_z^2 + c^2k_\perp^2$, in which the cutoff frequency $\omega_{co} = ck_\perp$ is dependent on the cavity cross section size and eigenmode. Because of the relatively small group velocity (0–0.3c) of the wave, as the resonance is close to the cutoff frequency, its frequency tuning range would be smaller. The HCIR offers two other advantages for a gyro-BWO. First, as it operates near the TE_{21} cutoff region it can generate a higher frequency for a given cavity cross section or allow a bigger cavity cross section for a given operating freqency. As the operating frequency increases to 1 THz the fundamental mode resonator has an aperture size 0.18 mm, but with this HCIR the size would be 0.3 mm. This would alleviate the difficulties in accurate machining and beam alignment in the cavity. Second, this TE_{21}-like eigenwave can efficiently interact with the 2nd harmonic of the electron cyclotron frequency without parasitic

oscillation; hence, the required magnetic field can be reduced by half. For example, at 1 THz, it reduces the required magnetic field from 40 to 20 T. In this experiment a frequency tuning range of 88–102.5 GHz was measured by tuning the applied magnetic field from 1.66 to 2.06 T.

The measured dispersion properties of the HCIR in comparison to the results from numerical simulation using the 3D particle-in-cell (PIC) code MAGIC [26] are shown in Fig. 2(a). The dispersion of the operating eigenwave was measured by determining its optical length as a function of frequency by using a vector network analyzer (VNA) (Anritsu ME7808). In the simulation the operating eigenwave was generated by injecting a left-hand circularly polarized wave into a right-handed HCIR at each frequency. A transverse component of the electric field inside the HCIR was measured along the axial direction. The measured field profile was then fast-Fourier-transform (FFT) analyzed so that the axial wave number of the eigenwave was obtained for each frequency.

Frequency tuning of the gyro-BWO can be achieved by shifting the electron cyclotron line upwards or downwards by adjusting either the operating magnetic field or electron energy (inherently from the expression of ω_c, tuning through the magnetic field is more sensitive and has larger range). Because of the nonsymmetrical geometry of the helical interaction region, the electron beam interacts only with the wave in one rotation; however, the wave could be in either the backward or forward direction. Upshifting of the electron cyclotron line would eventually give rise to the intersection of the beam line with a forward wave TE_{21} mode, i.e., normal gyrotron operation, as represented by the point 3 in Fig. 2(a). This reaches the upper limit of the frequency tuning range of the gyro-BWO. In this gyro-BWO, frequency tuning is achieved by adjusting the magnetic field while keeping the beam velocity ratio α unchanged.

In the experiment a stacked double-Blumlein pulsed high voltage source was used to provide the accelerating field. Fast electron beam diagnostics were constructed, having response times typically 5–20 ns, which permitted time correlated observation of the evolution of the pulse parameters. The electron accelerating potential was measured using a resistive voltage divider, while total electron emission current in the gun, typically 1.8 A when the cathode reached operating temperature, was measured using a current shunt in the anode earth connection. A 380 ns nearly flat-topped 40 kV voltage pulse was produced, having a rise time of 30–35 ns. The beam current was measured at the cavity using a Faraday cup, inserted into the beam tube. This beam current of 1.5 A was measured at the normal operating cathode temperature, although it was variable by adjusting the heating power applied to the cathode.

The radiation of the gyro-BWO can be coupled out at two positions. One is from the output coupler at the upstream side of the electron beam, the other through the output window at the downstream end. To verify and characterize the operation of the gyro-BWO, the millimeter wave pulse duration and temporal profile from the latter downstream end were obtained from a W-band crystal detector signal observed on a digital oscilloscope, time correlated with the electron-beam current and voltage profiles. A 350 ns microwave pulse was observed, rising 30 ns after the start of the electron beam pulse and terminating with its end. Typical recorded traces of the beam voltage, current, and the output millimeter wave are shown in Fig. 3.

A heterodyne frequency diagnostic was used to measure the frequency of the output radiation of the gyro-BWO. An in-band fundamental mixer (Millitech MXP-10-R) and a local oscillator signal produced from a 95 GHz Gunn diode (Millitech GDM-10-1013IR) were used and the resultant intermediate frequency (IF) signal was recorded using a 20 GHz, deep memory digitizing oscilloscope (Agilent DSX-X 92004A). At a cavity magnetic field of 1.867 T, the recorded IF signal is also shown in Fig. 3. It is noticeable that the output frequency of the gyro-BWO was changing slightly during the pulse because the voltage was not completely stable in the pulse. In the measurement

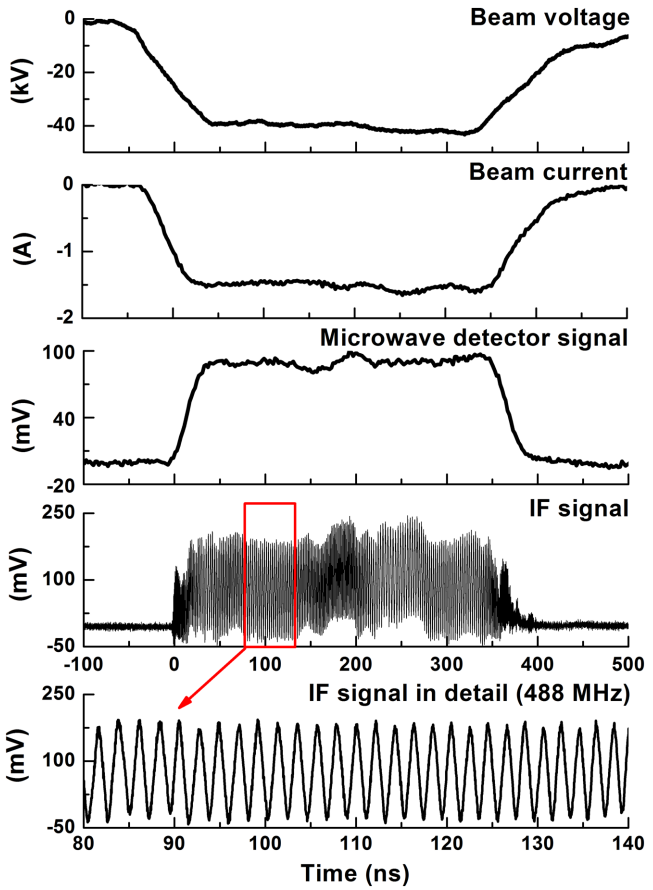

FIG. 3 (color online). Recorded beam accelerating potential, current, and terahertz signal and heterodyne IF signal from the gyro-BWO.

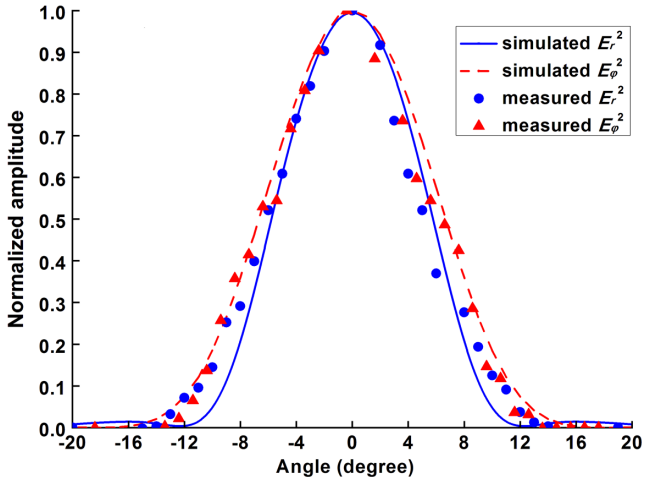

FIG. 4 (color online). Radial scan of far-field output radiation from measurement and simulation at 94 GHz.

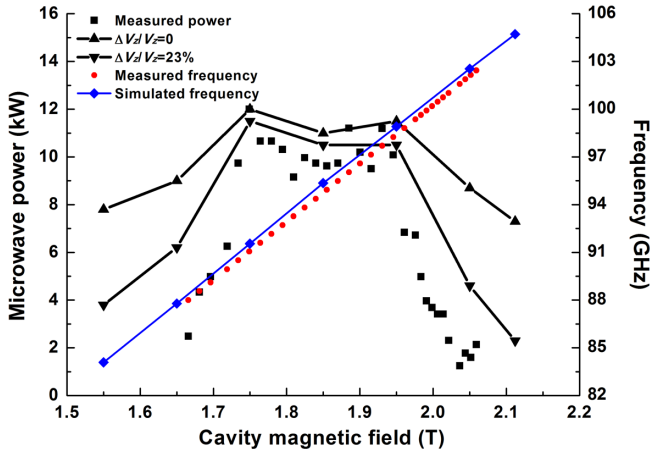

FIG. 5 (color online). Measured and simulated output frequency and power of the gyro-BWO as a function of tuning cavity magnetic field.

the output frequency of the gyro-BWO was obtained by FFT of the IF signal in the time period when the beam voltage was at 40 kV.

To verify the output mode was the TE_{11}, the far-field output radiation pattern from a conical antenna horn with an aperture diameter of ~20 mm was measured at 94 GHz output frequency. The radiation patterns associated with the radial and azimuthal E-field component were measured and are shown in Fig. 4 with a standard error of ±5% and a systematic error in the radial angle measurement of <2°. The far-field pattern was simulated using CST Microwave Studio and is also shown in Fig. 4 for comparison.

In order to measure the absolute power of the radiation pulse from the gyro-BWO, a 1.5 W, 90–97 GHz tunable signal was propagated into the gyro-BWO as a calibration source using the coupler. The radiation was then measured by a detector at a far-field point at the downstream window end. The whole transmission loss of the system was carefully measured by the VNA to be ~6 dB. By comparing the detector output from the gyro-BWO experiment and the calibration signal the output power of the gyro-BWO could be measured accurately.

At a beam energy of 40 keV and current of 1.5 A, the output frequency and power from the gyro-BWO was measured as a function of the tuning cavity magnetic field and is shown in Fig. 5. To complement the experimental investigations, the 3D PIC simulation code MAGIC was used to simulate the nonlinear beam-wave interaction of the gyro-BWO. An electron beam with parameters similar to that measured in the experiment was used, i.e., beam energy, current, and beam velocity ratio. As a comparison, the simulated output frequency and power of the gyro-BWO at an axial velocity spread of 0% and 23% are also shown in Fig. 5. From the simulation the axial velocity spread can be seen to have a small effect on the efficiency of the beam-wave interaction in the B field range of 1.75–1.95 T, but its effect becomes more evident at larger B field values. By comparing the measured and simulated output power we can assume the actual axial velocity spread of the beam was more than 23%. There was also a systematic discrepancy of ~0.4 GHz between the measured and simulated frequency. This could be an error from either the MAGIC simulation or the measurement of the driving current of the cavity coil which has an accuracy of ±0.5%.

In this millimeter wave gyro-BWO experiment stable output frequency and power were demonstrated due to single mode operation. A maximum output power of 12 kW, which corresponds to a 20% interaction efficiency was achieved with a 1.5 A, 40 kV large orbit electron beam. A wide frequency tuning range of 88–102.5 GHz was achieved by tuning the cavity magnetic field. Excellent agreement was shown between the simulations of the gyro-BWO using MAGIC and the measured results in the experiments. This method can, in principle, be extended to the higher terahertz range.

The authors would like to thank EPSRC UK (research Grant No. EP/G036659/1) for supporting this work and Dr. Peter Huggard and Mr. Mat Beardsley of the Millimetre Wave Technology Group at the STFC Rutherford Appleton Laboratory, UK for the construction of the HCIR. The EPSRC Engineering Loan Pool and Mr. Alan Ruddell are thanked for access to the Anritsu ME7808.

[1] K. R. Chu, Rev. Mod. Phys. **76**, 489 (2004).
[2] M. Einat, M. Pilossof, R. Ben-Moshe, H. Hirshbein, and D. Borodin, Phys. Rev. Lett. **109**, 185101 (2012).
[3] J. R. Sirigiri, K. E. Kreischer, J. Machuzak, I. Mastovsky, M. A. Shapiro, and R. J. Temkin, Phys. Rev. Lett. **86**, 5628 (2001).
[4] N. S. Ginzburg, I. V. Zotova, A. S. Sergeev, V. Yu. Zaslavsky, and I. V. Zheleznov, Phys. Rev. Lett. **108**, 105101 (2012).

[5] M. Yu. Glyavin, A. G. Luchinin, and G. Yu. Golubiatnikov, Phys. Rev. Lett. **100**, 015101 (2008).
[6] V. L. Bratman, Yu. K. Kalynov, and V. N. Manuilov, Phys. Rev. Lett. **102**, 245101 (2009).
[7] M. Tonouchi, Nat. Photonics **1**, 97 (2007).
[8] H. Park *et al.*, Rev. Sci. Instrum. **75**, 3787 (2004).
[9] K. B. Cooper, R. J. Dengler, G. Chattopadhyay, E. Schlecht, J. Gill, A. Skalare, I. Mehdi, and P. H. Siegel, IEEE Microw. Wirel. Compon. Lett. **18**, 64 (2008).
[10] L. R. Becerra, G. J. Gerfen, R. J. Temkin, D. J. Singel, and R. G. Griffin, Phys. Rev. Lett. **71**, 3561 (1993).
[11] G. S. Nusinovich and O. Dumbrajs, IEEE Trans. Plasma Sci. **24**, 620 (1996).
[12] S. Y. Park, R. H. Kyser, C. M. Armstrong, R. K. Parker, and V. L. Granatstein, IEEE Trans. Plasma Sci. **18**, 321 (1990).
[13] C. S. Kou, S. G. Chen, L. R. Barnett, H. Y. Chen, and K. R. Chu, Phys. Rev. Lett. **70**, 924 (1993).
[14] T. A. Spencer, R. M. Gilgenbach, and J. J. Choi, J. Appl. Phys. **72**, 1221 (1992).
[15] S. H. Chen, K. R. Chu, and T. H. Chang, Phys. Rev. Lett. **85**, 2633 (2000).
[16] M. A. Basten, W. C. Guss, K. E. Kreischer, R. J. Temkin, and M. Caplan, Int. J. Infrared Millim. Waves **16**, 889 (1995).
[17] C. L. Hung, M. F. Syu, M. T. Yang, and K. L. Chen, Appl. Phys. Lett. **101**, 033504 (2012).
[18] W. He, C. G. Whyte, E. G. Rafferty, A. W. Cross, A. D. R. Phelps, K. Ronald, A. R. Young, C. W. Robertson, D. C. Speirs, and D. H. Rowlands, Appl. Phys. Lett. **93**, 121501 (2008).
[19] C. R. Donaldson, W. He, A. W. Cross, F. Li, A. D. R. Phelps, L. Zhang, K. Ronald, C. W. Robertson, C. G. Whyte, and A. R. Young, Appl. Phys. Lett. **96**, 141501 (2010).
[20] C. R. Donaldson, W. He, L. Zhang, and A. W. Cross, IEEE Microw. Wirel. Compon. Lett. (to be published).
[21] L. Zhang, C. R Donaldson, and W. He, J. Phys. D **45**, 345103 (2012).
[22] L. Zhang, W. He, K. Ronald, A. D. R. Phelps, C. G. Whyte, C. W. Robertson, A. R. Young, C. R. Donaldson, and A. W. Cross, IEEE Trans. Microw. Theory Tech. **60**, 1 (2012).
[23] A. W. Cross, W. He, A. D. R. Phelps, K. Ronald, C. G. Whyte, A. R. Young, C. W. Robertson, E. G. Rafferty, and J. Thomson, Appl. Phys. Lett. **90**, 253501 (2007).
[24] W. He, A. W. Cross, A. D. R. Phelps, K. Ronald, and C. G. Whyte, E. G. Rafferty, C. W. Robertson, J. Thomson, S. V. Samsonov, V. L. Bratman, and G. G. Denisov, Appl. Phys. Lett. **89**, 091504 (2006).
[25] S. V. Samsonov, A. D. R. Phelps, V. L. Bratman, G. Burt, and G. G. Denisov, A. W. Cross, K. Ronald, W. He, and H. Yin, Phys. Rev. Lett. **92**, 118301 (2004).
[26] T. Gray, D. N. Smithe, and L. D. Ludeking, *Introduction to MAGIC* (Mission Research Corporation, Newington, VA, 2003).